Nonlinear Dyn (2015) 81:425–435
DOI 10.1007/s11071-015-2002-8

ORIGINAL PAPER

Nonlinear energy sink to control elastic strings: the internal resonance case

Angelo Luongo · Daniele Zulli

Received: 14 October 2014 / Accepted: 23 February 2015 / Published online: 6 March 2015

Abstract The use of nonlinear energy sink as a passive control device is extended here to a nonlinear elastic string, in internal resonance conditions, excited by an external harmonic force. The Multiple Scale/Harmonic Balance Method is directly applied to the partial differential equations ruling the dynamics of the system. The internal resonance condition of the string involves a rich response containing essentially both the resonant, directly excited, mode and a superharmonic one. Numerical results on a case study are presented.

Keywords Nonlinear energy sink · Infinite dimensional system · Internal resonance · Multiple Scale/Harmonic Balance Method

1 Introduction

Nonlinear energy sink (NES) is an essentially nonlinear oscillator which is used as passive control device. Its main feature, due to the lack of linear stiffness, is the capability of getting tuned to the primary structure in a wide range of frequencies, representing a considerable asset to the passive control performance, and overtaking the intrinsic limitations of more common devices such as tuned mass damper [1–3]. An extensive study on the use of NES is given in [4], where analytical, numerical and experimental verification on the characteristics of such a device is provided. There and in many other papers, the analytical studies are carried out by means of the application of the Complexification Averaging Method (CX-A, see [5]). Under this framework, in [6], a main linear oscillator excited by a harmonic force and equipped with NES is studied; in [7], an internally resonant two-d.o.f. system is considered as primary structure, still under the application of harmonic excitation; in [8,9], the use of NES is extended to aeroelastic problems, in order to suppress or reduce oscillations induced by wind. Discussion on energy pumping between linear and essentially nonlinear oscillators such as NES is given in [10,11], while extension of the use of NES to control non-ideal main structures are presented in [12,13]. NES attached to continuum primary linear structures, such as beams or plates, is considered in [14–19]. The possible occurrence of multiple coexisting solutions, sometimes thwarting the beneficial effects of the NES as control device in single-d.o.f. systems, is discussed in [20,21].

Other analytical studies of oscillators endowed with NES make use of the combination of the Multiple Scale Method and the Harmonic Balance (referred as MSHBM): the case of multi-d.o.f. dynamical systems under harmonic external force is considered in [22]; a

This work has been supported by the Italian Ministry of University (MIUR) through a PRIN 2010–2012 program (2010MBJK5B).

A. Luongo (✉) · D. Zulli
M&MoCS - University of L'Aquila, Via Giovanni Gronchi, 18, 67100 L'Aquila, AQ, Italy
e-mail: angelo.luongo@univaq.it

two-d.o.f. nonlinear airfoil under wind effects is analyzed in [23]; the chatter in the turning process is studied in [24]; lateral vibrations of a rotor are evaluated in [25]. In [26], a nonlinear elastic string under harmonic force is considered when a NES is attached at a certain position of the span, and the internally nonresonant case is analyzed, being the string supported at one end by a mass-spring system which detunes the first few natural frequencies. There, as well as in [22,23], the lacking of internal resonance causes the dynamics of the principal structure to be described by just one active mode, while all the other modes turn out to be passive. Moreover, in [26], the perturbation scheme is applied in direct approach, i.e., the Multiple Scale Method is directly imposed on the partial differential equations, as done (for systems without NES) in [27–31].

In this paper, the analysis of [26] is extended to internally resonant taut strings. The same model of [26] is used, except for the right boundary condition, where a fixed support is now considered, which entails the typical internal resonance conditions among the infinite natural frequencies of the string to occur. As it was discussed in [28], when NES is absent, the dominant dynamics of a nonlinear, double supported, taut string under harmonic excitation resonant to a generic mode (say the rth), is ruled just by the resonant (rth) mode itself, while the amplitudes of the infinite remaining modes give higher-order contribution. The effect of the NES on this peculiar behavior is discussed here, further extending the MSHBM to systems which include internal resonances, possibly involving more than one active mode of the principal structure. Relevant amplitude modulation equations are obtained and some numerical results are reported, compared to those provided by integration of the system after the application of a multi-mode Galerkin projection.

2 The model

A double supported extensible elastic string is considered here, as shown in Fig. 1. Its initial length is ℓ and prestress tensile force N, and an external force, ruled by the law $f(x,t) = p(x)\cos(\Omega t)$, is applied along the span. Here x is the abscissa measured in the prestressed configuration and t is the time. The linear mass density is ρ and the axial stiffness is EA. The equations of motion of the string are taken from [27,28,32]: they are valid for moderately large displacements, under

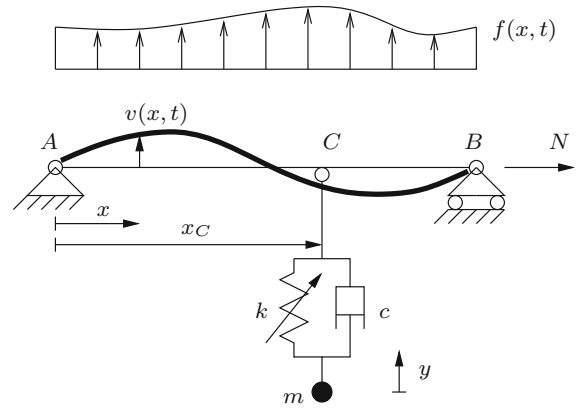

Fig. 1 String equipped with a NES

the hypothesis that the longitudinal versus transverse celerity-rate is large. A NES is applied to the string at point C, corresponding to the abscissa x_C. The mass of the NES is m, its linear damping c and cubic stiffness k. The in-plane transverse displacement of a generic point of the string is $v(x,t)$ while the displacement of the mass of the NES is $y(t)$. The equations read:

$$\begin{aligned} &N v''(x,t) + \frac{EA}{\ell} v''(x,t) \left[\int_0^\ell \frac{v'^2(x,t)}{2} \mathrm{d}x \right] - \rho \ddot{v}(x,t) \\ &\quad + p(x)\cos(\Omega t) - \Big[k(v(x,t) - y(t))^3 \\ &\quad + c(\dot{v}(x,t) - \dot{y}(t)) \Big] \delta(x - x_C) = 0 \\ &\quad m\ddot{y}(t) - \Big[k(v(x_C,t) - y(t))^3 \\ &\quad + c(\dot{v}(x_C,t) - \dot{y}(t)) \Big] = 0 \end{aligned} \tag{1}$$

where $\delta(x)$ is the Dirac delta, the dot indicates time-derivative and the prime space-derivative.

The geometric boundary conditions at the supports read

$$\begin{aligned} v(0,t) &= 0 \\ v(\ell,t) &= 0 \end{aligned} \tag{2}$$

Relevant initial conditions must be added too.

Nondimensional quantities are defined as:

$$\begin{aligned} &\tilde{x} = \frac{x}{\ell},\ \tilde{t} = \bar{\omega} t,\ \tilde{y} = \frac{y}{L},\ \tilde{v} = \frac{v}{L},\ \tilde{x}_C = \frac{x_C}{\ell}, \\ &\tilde{\delta} = \ell\delta,\ \tilde{p} = \frac{p\ell}{N}\sqrt{\frac{\mathrm{EA}}{N}},\ \tilde{\Omega} = \frac{\Omega}{\bar{\omega}}, \\ &\kappa = \frac{k\ell^3}{\mathrm{EA}},\ \xi = \frac{c}{\sqrt{\rho N}},\ \tilde{m} = \frac{m}{\rho\ell} \end{aligned} \tag{3}$$

where L is a characteristic length defined as $L := \ell\sqrt{\frac{N}{\mathrm{EA}}}$, and $\bar{\omega} = \frac{1}{\ell}\sqrt{\frac{N}{\rho}}$. After the substitutions of

the definitions (3) in Eq. (1), the nondimensional version of the equations of motion is obtained. Omitting the tilde, including the contribution of linear structural damping ($\zeta \dot{v}(x,t)$, where ζ is the damping coefficient), and introducing the relative displacement between the main structure at point C and NES, namely $z(t) := v(x_C,t) - y(t)$, Eq. (1) become

$$\begin{aligned} &\ddot{v} + \zeta\dot{v} - v'' - v''\left[\int_0^1 \frac{v'^2}{2}\mathrm{d}x\right] \\ &\quad + \left[\kappa z^3 + \xi\dot{z}\right]\delta(x - x_C) = p\cos(\Omega t) \\ &\quad m(\ddot{z} - \ddot{v}_C) + \kappa z^3 + \xi\dot{z} = 0 \end{aligned} \tag{4}$$

where $v_C(t) := v(x_C,t)$, and the boundary conditions

$$\begin{aligned} v(0,t) &= 0 \\ v(1,t) &= 0 \end{aligned} \tag{5}$$

where the dot and the prime stand here for differentiation with respect to the nondimensional time and abscissa, respectively.

3 The Multiple Scale/Harmonic Balance Method

In order to obtain the perturbation equations, the procedure described in [26] is used here; it is briefly recalled for the sake of completeness. A nondimensional small parameter ϵ is introduced to rescale the dependent variables and the parameters: the displacements are $(v,z) := \epsilon^{1/2}(\tilde{v},\tilde{z})$, consistently with the presence of cubic nonlinearity; the damping factor is $\zeta = \epsilon\tilde{\zeta}$ and the external force is $p = \epsilon^{3/2}\tilde{p}$, consistently with the idea to let both the terms appear at the same level of the nonlinearity. The external excitation is considered 1:1 resonant with one of the linear modes (the rth, of frequency $\omega_r = r\pi$) of the string with NES disengaged. A detuning parameter σ is introduced for the external excitation, as $\Omega = \omega_r + \sigma$; it is rescaled as $\sigma = \epsilon\tilde{\sigma}$. The parameters of the NES are rescaled too, since both its mass and damping are assumed small: $(m,\xi) := \epsilon(\tilde{m},\tilde{\xi})$. After the application of the rescaling, the omission of tilde and division by $\epsilon^{1/2}$, Eq. (4) become:

$$\begin{aligned} &\ddot{v} - v'' + \epsilon\left[\zeta\dot{v} - v''\left[\int_0^1 \frac{v'^2}{2}\mathrm{d}x\right]\right. \\ &\quad \left. + [\kappa z^3 + \xi\dot{z}]\delta(x - x_C) - p\cos(\Omega t)\right] = 0 \\ &\quad \epsilon[m(\ddot{z} - \ddot{v}_C) + \kappa z^3 + \xi\dot{z}] = 0 \end{aligned} \tag{6}$$

Independent time scales $t_0 := t$, $t_1 := \epsilon t$, $t_2 = \epsilon^2 t, \ldots$ are introduced and the relevant derivatives are expressed as $\frac{\partial}{\partial t} = d_0 + \epsilon d_1 + \epsilon^2 d_2 + \cdots$ and $\frac{\partial^2}{\partial t^2} = d_0^2 + 2\epsilon d_0 d_1 + \epsilon^2(d_1^2 + 2d_0 d_2) + \cdots$, where $d_j := \partial/\partial t_j$, for $j = 0, 1, 2, \ldots$. Series expansion of the dependent variables is applied as:

$$\begin{Bmatrix} v \\ z \end{Bmatrix} = \begin{Bmatrix} v_0 \\ z_0 \end{Bmatrix} + \epsilon \begin{Bmatrix} v_1 \\ z_1 \end{Bmatrix} + \epsilon^2 \begin{Bmatrix} v_2 \\ z_2 \end{Bmatrix} + \cdots \tag{7}$$

After substitution in Eq. (6) and boundary conditions, the collection of terms at the same order in ϵ gives the perturbation equations:

order ϵ^0 :

$$d_0^2 v_0 - v_0'' = 0 \tag{8}$$

order ϵ^1 :

$$\begin{aligned} &d_0^2 v_1 - v_1'' = -2d_0 d_1 v_0 - \zeta d_0 v_0 + p\cos(\Omega t_0) \\ &\quad -(\xi d_0 z_0 + \kappa z_0^3)\delta(x - x_C) + v_0''\left[\int_0^1 \frac{v_0'^2}{2}\mathrm{d}x\right] \end{aligned} \tag{9}$$

$$m(d_0^2 z_0 - d_0^2 v_{C_0}) + \xi d_0 z_0 + \kappa z_0^3 = 0 \tag{10}$$

order ϵ^2:

$$\begin{aligned} &d_0^2 v_2 - v_2'' = -(d_1^2 v_0 + 2d_0 d_2 v_0 + 2d_0 d_1 v_1) \\ &\quad -\zeta(d_2 v_0 + d_1 v_1) - \left[\xi(d_0 z_1 + d_1 z_0) + 3\kappa z_0^2 z_1\right] \\ &\quad \delta(x - x_C) + v_1''\left[\int_0^1 \frac{v_0'^2}{2}\mathrm{d}x\right] + v_0''\left[\int_0^1 v_0' v_1'\mathrm{d}x\right] \end{aligned} \tag{11}$$

$$\begin{aligned} &m(d_0^2 z_1 - d_0^2 v_{C_1}) + \xi d_0 z_1 + 3\kappa z_0^2 z_1 \\ &\quad = -2m(d_0 d_1 z_0 - d_0 d_1 v_{C_0}) - \xi d_1 z_0 \end{aligned} \tag{12}$$

At any order, the boundary conditions are trivial:

order ϵ^k :

$$\begin{aligned} v_k(0, t_0, t_1, \ldots) &= 0, \\ v_k(1, t_0, t_1, \ldots) &= 0 \end{aligned} \tag{13}$$

for $k = 0, 1, 2$. So far, except for the boundary condition at the point B, the perturbation equations are identical to those reported in [26] and valid for the internally nonresonant case. It should be noted that no equation relevant to the NES appears at order ϵ^0, where just the linearized problem of the string (with NES disengaged) is retained. This occurrence is due to the small value of mass and damping of the NES, as well as to the fact that its stiffness is essentially nonlinear. The solution of Eqs. (8) and (13), which represents the generating solution of the perturbation procedure, should contain all the infinite components relevant to the infinite

eigenfunction of the linear system (see [28]). However, driven by inspection of the shape of the equations of motion and by the presence in them of the cubic nonlinearity, and being aimed at obtaining approximated solutions for the system, just the resonant ($j = r$) and a superharmonic ($j = s := 3r$) components are chosen to be retained in the solution:

$$v_0(x, t_0, t_1, \ldots) = A_r(t_1, \ldots)\varphi_r(x)e^{i\omega_r t_0} + A_s(t_1, \ldots)\varphi_s(x)e^{i\omega_s t_0} + cc \quad (14)$$

where: $A_j(t_1, \ldots)$ are the complex modal amplitudes to be evaluated, depending on the slower timescales; i is the imaginary unit; $\omega_j = j\pi$ and $\varphi_j(x) = \sin(\omega_j x)$ are the jth eigenvalue and (real) eigenfunction of the problem with NES disengaged; cc stands for complex conjugate ($j = r, s$).

Passing at order ϵ, the Harmonic Balance method [27] is applied to the NES Eq. (10), assuming as solution for it a one-term Fourier expansion:

$$z_0(t_0, t_1, \ldots) = B_{0_r}(t_1, \ldots)e^{i\omega_r t_0} + cc \quad (15)$$

where $B_{0_r}(t_1, \ldots)$ is the complex amplitude depending on slower time scales, to be evaluated. The substitution of Eqs. (14) and (15) in Eq. (10) and the balance of frequency ω_r is carried out while, still in the idea of approximation, other frequencies are neglected (see [22] for a discussion on the contribution of higher frequencies). The procedure gives rise to the following algebraic equation:

$$-m\omega_r^2(B_0 - A_r\varphi_r(x_c)) + i\xi\omega_r B_0 + 3\kappa B_0^2\bar{B}_0 = 0 \quad (16)$$

where the overbar stands for complex conjugate. To obtain the real form of Eq. (16), the following steps are covered: (a) application of the polar transformation for both A_r and B_0, which reads $A_r := \frac{1}{2}a_r e^{i\alpha_r}$ and $B_0 := \frac{1}{2}be^{i\beta}$; (b) separation of real and imaginary parts; (c) squaring and adding the two obtained parts. The equation for the invariant manifold which describes a first approximation of a Nonlinear Normal Mode of the system is therefore written:

$$m^2\omega_r^4\varphi_r(x_c)^2a_r^2 = \left(m\omega_r^2 b - \frac{3}{4}\kappa b^3\right)^2 + \xi^2\omega_r^2 b^2 \quad (17)$$

The dynamics outside the manifold (17) is ruled by the equations of the string at the same order, namely Eqs. (9) and (13) as well as the NES equation at the order ϵ^2, which will be tackled ahead. In particular, the solution of Eq. (9) is sought in the form

$$\begin{aligned} v_1(x, t_1, t_2) = {} & \psi_r(x, t_1, t_2)e^{i\omega_r t_0} + \psi_s(x, t_1, t_2)e^{i\omega_s t_0} \\ & + \psi_{2s-r}(x, t_1, t_2)e^{i\omega_{2s-r} t_0} \\ & + \psi_{2s+r}(x, t_1, t_2)e^{i\omega_{2s+r} t_0} \\ & + \psi_{3s}(x, t_1, t_2)e^{i\omega_{3s} t_0} + cc \end{aligned} \quad (18)$$

where $\psi_q(x, t_1, t_2)$ are complex functions to be determined ($q = r, s, 2s-r, 2s+r, 3s$). This expression for v_1 in Eq. (19) is suggested by the presence of cubic nonlinear terms in Eq. (9) but, in the spirit of the approximation, just components in $q = r, s$ are actually retained, while the other terms are considered as higher-order harmonics. Then, Eq. (18) is replaced by

$$\begin{aligned} v_1(x, t_1, t_2) = {} & \psi_r(x, t_1, t_2)e^{i\omega_r t_0} \\ & + \psi_s(x, t_1, t_2)e^{i\omega_s t_0} + cc \end{aligned} \quad (19)$$

and substituted in Eqs. (9) and (13), and terms multiplying $\exp(i\omega_r t_0)$ and $\exp(i\omega_s t_0)$ are separated, giving two ordinary differential equations with relevant boundary conditions, respectively. They read:

$$\psi_j'' + \omega_j^2\psi_j = -f_j(x, t_1, t_2) \quad (20)$$

with boundary conditions

$$\begin{aligned} \psi_j(0, t_1, t_2) &= 0 \\ \psi_j(1, t_1, t_2) &= 0 \end{aligned} \quad (21)$$

where

$$\begin{aligned} f_j(x, t_1, t_2) := {} & -2i\omega_j\varphi_j(x)d_1A_j - i\zeta\omega_j\varphi_j(x)A_j \\ & -[(i\omega_j\xi B_0 + 3\kappa B_0^2\bar{B}_0)\Delta_{j,r} + \kappa B_0^3\Delta_{j,s}]\delta(x - x_C) \\ & + \left[A_r\varphi_r''(x)\sum_{h=r,s}A_h\bar{A}_h\int_0^1\varphi_h'(x)^2\mathrm{d}x\right. \\ & \left. + \left(\frac{A_r^2\bar{A}_r}{2}\varphi_r''(x) + \frac{A_s\bar{A}_r^2}{2}\varphi_s''(x)\right)\int_0^1\varphi_r'(x)^2\mathrm{d}x\right]\Delta_{j,r} \\ & + \left[\left(\frac{A_r^3}{2}\varphi_r''(x) + A_sA_r\bar{A}_r\varphi_s''(x)\right)\int_0^1\varphi_r'(x)^2\mathrm{d}x\right. \\ & \left. + \left(\frac{A_s\bar{A}_s^2}{2}\varphi_s''(x) + A_s^2\bar{A}_s\varphi_s''(x)\right)\int_0^1\varphi_s'(x)^2\mathrm{d}x\right]\Delta_{j,s} \\ & + \frac{p(x)}{2}e^{i\sigma t_1}\Delta_{j,r} \end{aligned} \quad (22)$$

and

$$\Delta_{j,h} = \begin{cases} 1 & j = h \\ 0 & j \neq h \end{cases} \quad (23)$$

for $j = r, s$.

In order to get a not diverging solution from Eqs. (20) and (21), the solvability condition must be enforced on them, which reads:

$$\int_0^1 f_j(x,t_1,t_2)\varphi_j(x)\mathrm{d}x = 0 \tag{24}$$

Substitution of Eq. (22) in Eq. (24) for $j = r, s$ provides:

$$\begin{aligned} d_1 A_r &= -\frac{\zeta}{2}A_r - \left[\xi B_0 - \frac{3i\kappa}{\omega_r}B_0^2\bar{B}_0\right]\varphi_r(x_C) \\ &\quad + i\frac{\omega_r}{4}A_r\left[\frac{3}{2}\omega_r^2 A_r\bar{A}_r + \omega_s^2 A_s\bar{A}_s\right] - \frac{ip_r}{2\omega_r}e^{i\sigma t_1} \\ d_1 A_s &= -\frac{\zeta}{2}A_s - \frac{i\kappa}{\omega_s}B_0^3\varphi_r(x_C) \\ &\quad + i\frac{\omega_s}{4}A_s\left[\omega_r^2 A_r\bar{A}_r + \frac{3}{2}\omega_s^2 A_s\bar{A}_s\right] \end{aligned} \tag{25}$$

where $p_r = \int_0^1 p(x)\varphi_r(x)\mathrm{d}x$. It is worth noticing that the external force contribution p_r appears just in the equation ruling the resonant amplitude A_r [Eq. (25a)]. Moreover, the single component B_0 of the NES amplitude of relative oscillation appears in both the equations (25a, b). However, it would not appear in equations relevant to amplitudes A_j, for $j \neq r, s$, if those amplitudes were considered in the generating solution (14). That means that the possible equations ruling all the other amplitudes different than A_r and A_s would give trivial solution for them ($A_j \to 0$, for $j \neq r, s$, as it happens for the string with NES disengaged for $j \neq r$ [28]), confirming the good choice of retaining just the resonant and superharmonic contributions. On the other hand, if a more precise solution for the NES oscillation z_0 were considered in (15), containing, e.g., the component r as well as the component s, they would couple the amplitude modulation equations relevant to string amplitudes of index $j = r, s, 2s-r, 2s+r, 3s$, which in this case should be retained in the generating solution (14).

The substitution of Eq. (25) in Eqs. (20) and (21) allows one to obtain a solution for this system, which reads:

$$\begin{aligned} \psi_r(x,t_1) &= -\frac{\omega_r^2\omega_s^2}{4}A_s\bar{A}_r^2 J_{rs}(x) \\ &\quad + \left[i\xi\omega_r B_0 + 3\kappa B_0^2\bar{B}_0\right][I_r(x,x_C) \\ &\quad - 2\varphi_r(x)J_r(x)] - \left[\frac{P_r(x)}{2} - p_r J_r(x)\right]e^{i\sigma t_1} \\ \psi_s(x,t_1) &= \kappa B_0^3(I_s(x,x_C) - 2\varphi_s(x)J_s(x)) \\ &\quad - \frac{\omega_r^4}{4}A_r^3 J_{rs}(x) \end{aligned} \tag{26}$$

where

$$\begin{aligned} I_j(x,x_C) &= \frac{1}{\omega_j}\sin(\omega_j(x-x_C))H(x-x_C) \\ J_j(x) &= \frac{1}{2\omega_j}(\sin(\omega_j x) - \omega_j x\cos(\omega_j x)) \\ J_{rs}(x) &= \frac{\omega_r\sin(\omega_s x) - \omega_s\sin(\omega_r x)}{\omega_r(\omega_r^2-\omega_s^2)} \\ P_r(x) &= \frac{1}{\omega_r}\int_0^x p(\theta)\sin(\omega_r(x-\theta))\mathrm{d}\theta \end{aligned} \tag{27}$$

and $H(x)$ is the Heaviside step (Dirac delta and Heaviside step are used in the paper in the sense of the distributions). In Eq. (26), the normalization condition consisting in a vanishing amplitude for the complementary solution is assumed.

Equation (12) is considered and a further harmonic balance is applied to it, still assuming a one-term Fourier expansion for z_1:

$$z_1(t_0,t_1,\ldots) = B_1(t_1,\ldots)e^{i\omega_r t_0} + cc \tag{28}$$

Substituting Eqs. (14), (15) and (19) in Eq. (12) and balancing frequency ω_r, the following equation is obtained:

$$\begin{aligned} &-m\left[\omega_r^2 B_1 - 2i\omega_r d_1 B_0 + 2i\omega_r\varphi_r(x_C)d_1 A_r\right] \\ &+ \xi d_1 B_0 + i\xi\omega_r B_1 + 3\kappa B_0^2\bar{B}_1 \\ &- m\frac{\omega_r^2\omega_s^2}{4}A_s\bar{A}_r^2 J_{rs}(x_C) \\ &- 2m\left[i\xi\omega_r B_0 + 3\kappa B_0^2\bar{B}_0\right]\varphi_r(x_C)J_r(x_c) \\ &- m\left[\frac{P_r(x_C)}{2} - p_r J_r(x_C)\right]e^{i\sigma t_1} = 0 \end{aligned} \tag{29}$$

Equations (16) and (29) can be reconstituted, using the definition $B := B_0 + \epsilon B_1$; coming back to the true time, reabsorbing ϵ for those and for Eq. (25) one obtains:

$$\begin{aligned} \dot{A}_r &= -\frac{\zeta}{2}A_r - \left[\xi B - \frac{3i\kappa}{\omega_r}B^2\bar{B}\right]\varphi_r(x_C) \\ &\quad + i\frac{\omega_r}{4}A_r\left[\frac{3}{2}\omega_r^2 A_r\bar{A}_r + \omega_s^2 A_s\bar{A}_s\right] - \frac{ip_r}{2\omega_r}e^{i\sigma t} \\ \dot{A}_s &= -\frac{\zeta}{2}A_s - \frac{i\kappa}{\omega_s}B^3\varphi_r(x_C) \\ &\quad + i\frac{\omega_s}{4}A_s\left[\omega_r^2 A_r\bar{A}_r + \frac{3}{2}\omega_s^2 A_s\bar{A}_s\right] \\ &\quad - 2i\omega_r m\varphi_r(x_C)\dot{A}_r + (\xi + 2i\omega_r m)\dot{B} \end{aligned}$$

$$
\begin{aligned}
&= -m\omega_r^2\varphi_r(x_C)A_r + (m\omega_r^2 - i\xi\omega_r)B \\
&\quad - 3\kappa B^2\bar{B} + m\frac{\omega_r^2\omega_s^2}{4}A_s\bar{A}_r^2 J_{rs}(x_C) \\
&\quad + 2m\left[i\xi\omega_r B_0 + 3\kappa B_0^2\bar{B}_0\right]\varphi_r(x_C)J_r(x_c) \\
&\quad + m\left[\frac{P_r(x_C)}{2} - p_r J_r(x_C)\right]e^{i\sigma t_1}
\end{aligned} \tag{30}
$$

Equation (30) are the complex amplitude modulation equations (AME) ruling the slow dynamics of the string and NES, also outside the manifold (16). The derivatives of B and A_r have been obtained at the second order, due to the fact that they are multiplied by small coefficients ξ and m. Equation (30) can be written in real form through the polar transformation $A_j(t) := \frac{1}{2}a_j(t)e^{i\alpha_j(t)}$ $(j = r, s)$ and $B(t) := \frac{1}{2}b(t)e^{i\beta(t)}$, separating real and imaginary parts, and defining phase differences as $\gamma(t) := \sigma t - \alpha_r(t)$, $\chi(t) := \alpha_s(t) + 3\gamma(t) - 3\sigma t$ and $\vartheta(t) := \sigma t - \beta(t)$. They read

$$
\begin{aligned}
&\dot{a}_r = \mathcal{F}_1(a_r, a_s, b, \gamma, \chi, \vartheta) \\
&\dot{a}_s = \mathcal{F}_2(a_r, a_s, b, \gamma, \chi, \vartheta) \\
&m\omega_r\dot{b} + m\omega_r a_r\dot{\gamma}\sin(\omega_r x_C)\sin(\gamma - \vartheta) \\
&\qquad - \frac{1}{2}\xi b\dot{\vartheta} - m\omega_r\dot{a}_r\sin(\omega_r x_C)\cos(\gamma - \vartheta) \\
&\quad = \mathcal{F}_3(a_r, a_s, b, \gamma, \chi, \vartheta) \\
&a_r\dot{\gamma} = \mathcal{F}_4(a_r, a_s, b, \gamma, \chi, \vartheta) \\
&a_s\dot{\chi} - 3a_s\dot{\gamma} = \mathcal{F}_5(a_r, a_s, b, \gamma, \chi, \vartheta) \\
&m\omega_r b\dot{\vartheta} - m\omega_r a_r\dot{\gamma}\sin(\omega_r x_C)\cos(\gamma - \vartheta) \\
&\qquad + \frac{1}{2}\xi\dot{b} - m\omega_r\dot{a}_r\sin(\omega_r x_C)\sin(\gamma - \vartheta) \\
&\quad = \mathcal{F}_6(a_r, a_s, b, \gamma, \chi, \vartheta)
\end{aligned} \tag{31}
$$

The nonlinear functions $\mathcal{F}_k$ $(k = 1, \ldots, 6)$ are reported in Appendix 1.

If one defines the columns $\mathbf{u} := \{a_r, a_s, b, \gamma, \chi, \vartheta\}$, $\mathcal{F} := \{\mathcal{F}_1, \mathcal{F}_2, \mathcal{F}_3, \mathcal{F}_4, \mathcal{F}_5, \mathcal{F}_6\}$ and the mass matrix $\mathcal{M}(\mathbf{u})$ (the expression of $\mathcal{M}(\mathbf{u})$ is reported in Appendix 1), Eq. (31) can be written as

$$
\mathcal{M}(\mathbf{u})\dot{\mathbf{u}} = \mathcal{F}(\mathbf{u}) \tag{32}
$$

which in normal form becomes (provided $\det(\mathcal{M}) \neq 0$)

$$
\dot{\mathbf{u}} = \mathcal{G}(\mathbf{u}) \tag{33}
$$

where $\mathcal{G}(\mathbf{u}) := \mathcal{M}(\mathbf{u})^{-1}\mathcal{F}(\mathbf{u})$

Equilibrium points of system (33), describing periodic motions of the variables $v(x, t)$ and $z(t)$, are evaluated by solving the same system for $\dot{a}_r = \dot{a}_s = \dot{b} = \dot{\gamma} = \dot{\vartheta} = \dot{\chi} = 0$, and their stability properties are detected looking at the real part of the eigenvalues of the Jacobian matrix; periodic solutions of Eq. (33), giving rise to quasiperiodic motions in $v(x, t)$ and $z(t)$, are numerically obtained through direct integration of Eq. (31), while semi-analytical detection of the bands of existence of the SMR (see e.g., [22]) is not carried out here as a consequence of the increased dimension of the system, which makes the procedure not computationally easy. The computations, carried out by means of the softwares Auto [33] and Mathematica [34], are presented in the following Section for a case study.

4 Numerical results

Numerical results are evaluated for a string of damping coefficient $\zeta = 1.119\,\%$ (the value is reconstructed from [35] where modal damping ratios are experimentally measured for a stay). The external force is assumed

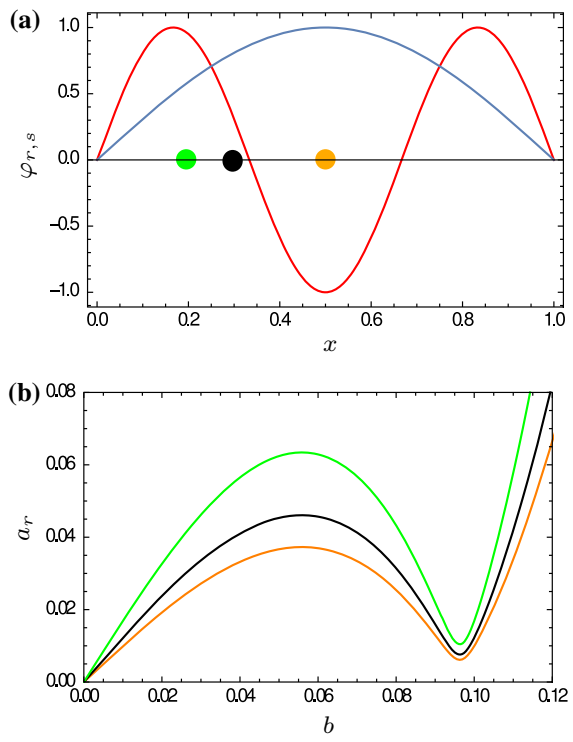

Fig. 2 Position of the NES on the span: $x_C = 0.5$, *orange point*; $x_C = 0.3$, *black point*; $x_C = 0.2$, *green point*; first mode (*blue line*) and third mode (*red line*) of the string (**a**); invariant manifolds corresponding to the three positions of the NES (**b**). (Color figure online)

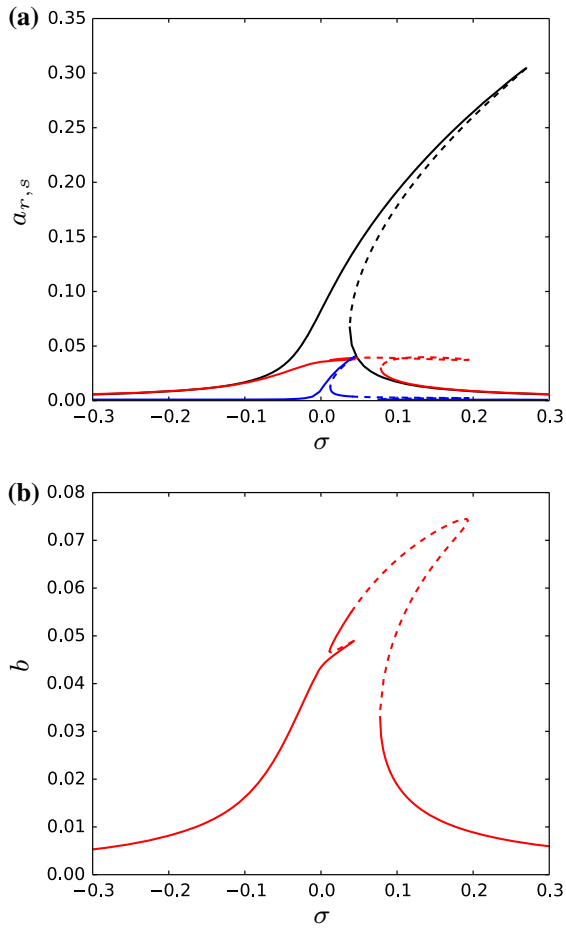

Fig. 3 Frequency–response curves: **a** amplitude a_r with NES disengaged (*black line*), amplitude a_r (*red line*) and a_s (*blue line*) with NES engaged; **b** amplitude of NES b (*red line*). Force $p = 0.0084$, position of the NES $x_C = 0.5$. *Continuous line* stable; *dashed line* unstable. (Color figure online)

as uniform ($p(x) \equiv p$), and the nondimensional parameters of the NES are $m = 0.05$, $\kappa = 70$, $\xi = 0.01$.

From now on, the external force is assumed to be resonant to the first mode, therefore $r = 1$, $s = 3$, moreover $\omega_r := \pi$, $\omega_s := 3\pi$ and $\varphi_r(x) := \sin(\pi x)$, $\varphi_s(x) = \sin(3\pi x)$.

The position of the NES along the span changes the invariant manifold (17) in the way shown in Fig. 2. In particular, if the NES is located at the mid-span (orange point in Fig. 2a, $x_C = 0.5$), which is the antinode of both the first and third modes (blue and red lines in Fig. 2a, respectively), for a fixed value of amplitude

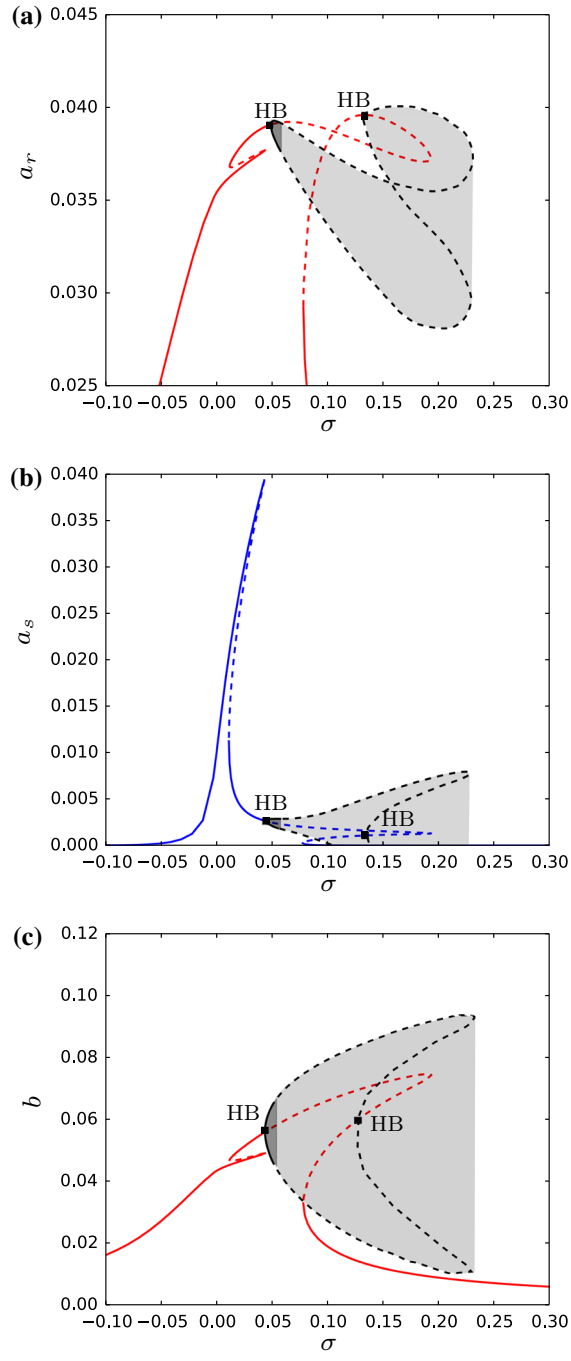

Fig. 4 Frequency–response curves of the amplitudes a_r (**a**), a_s (**b**) and b (**c**), for $p = 0.0084$ and $x_C = 0.5$. *Continuous line* stable; *dashed line* unstable. *Dark filled regions* stable quasiperiodic oscillations. *Light filled regions* unstable quasiperiodic oscillations

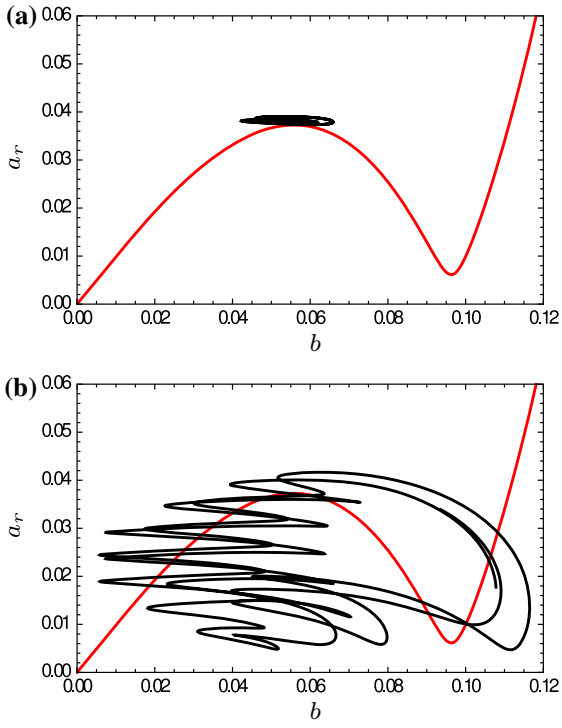

Fig. 5 Weakly modulated response [$\sigma = 0.048$, *black line* (**a**)] and strongly modulated response [$\sigma = 0.060$, *black line* (**b**)] with NES at the antinode, for $p = 0.0084$ and $x_C = 0.5$; *red line* invariant manifold. *Continuous line* stable; *dashed line* unstable. (Color figure online)

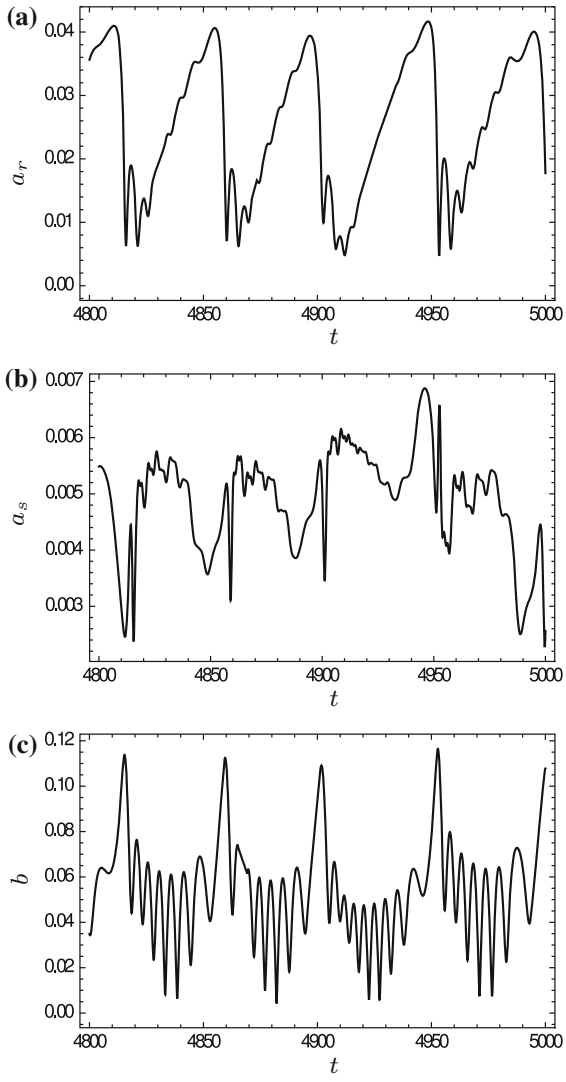

Fig. 6 Strongly modulated response ($\sigma = 0.06$, $p = 0.0084$, $x_C = 0.5$). Time evolution of a_r (**a**); time evolution of a_s (**b**); time evolution of b (**c**)

of oscillation b of the NES, a smaller amplitude of oscillation a of the principal structure occurs, than the case where the NES is elsewhere (i.e., the orange curve is always underneath the black and green ones, corresponding to $x_C = 0.3$ and $x_C = 0.2$ in Fig. 2a, respectively). Therefore, the NES is more capable to absorb energy from the main structure, which is the main objective of the control problem, when its position corresponds to the node of the mode shape.

Amplitude of periodic motions of both the string and NES, for force amplitude value $p = 0.0084$, are shown in Fig. 3. In Fig. 3a, the black line corresponds to the response a_r without NES, which is the unique contribution to the solution of the string; it is superimposed to the response curve obtained when NES is engaged, in terms of a_r (red line) and a_s (blue line). The strong reduction of the peak amplitude is evident, which is a beneficial effect of the NES, as well as the participation of the superharmonic component a_s to the dynamics. In Fig. 3b, the amplitude of oscillation b of the NES is shown.

A more detailed view of the same frequency–response curves is shown in Fig. 4. There, Hopf bifurcation points (HB) are highlighted; they induce the arising of quasiperiodic oscillations of the string and NES, which are stable close to the left HB point (dark filled regions) and representing weakly modulated responses (WMR). After secondary bifurcations, they become unstable (light filled regions) and the response jumps to Strongly Modulated Responses (which are not shown in the pictures). In Fig. 5, WMR and SMR (black lines) are shown as superimposed to the invariant manifold (red lines), for $\sigma = 0.046$ (WMR, Fig. 5a) and $\sigma = 0.060$

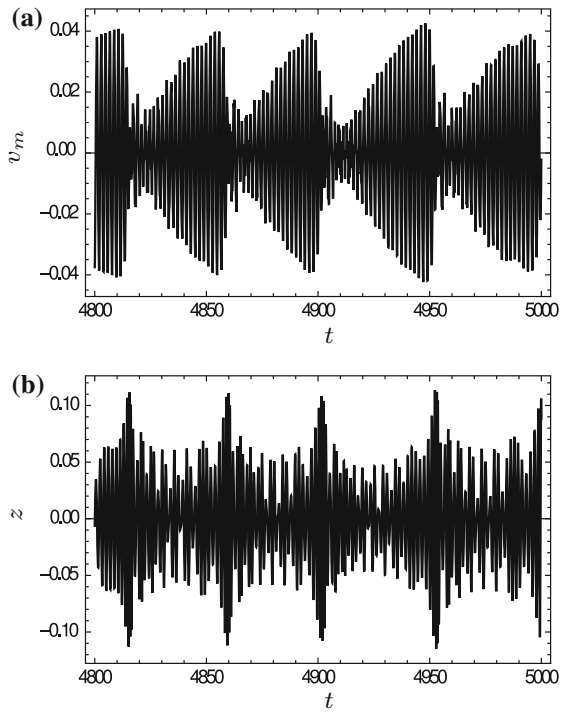

Fig. 7 Strongly modulated response ($\sigma = 0.06$, $p = 0.0084$, $x_C = 0.5$). Time evolution of v_m (**a**); time evolution of z (**b**)

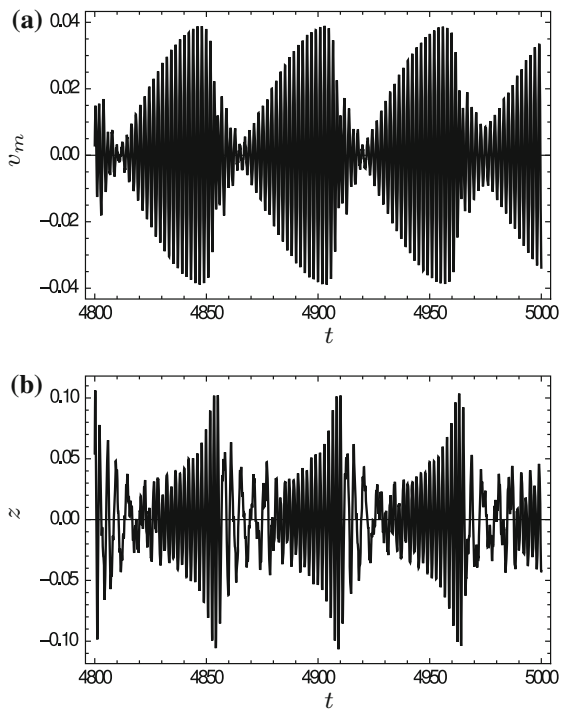

Fig. 8 Strongly modulated response from the Galerkin model ($\sigma = 0.06$, $p = 0.0084$, $x_C = 0.5$). Time evolution of v_m (**a**); time evolution of z (**b**)

(SMR, Fig. 5b). The time evolution of the same SMR is shown in Fig. 6, where the three components a_r, a_s and b experience relaxation oscillations. In Fig. 7, the reconstituted displacement of the midpoint of the string ($v_m := v(1/2, t)$) and of the NES ($z(t)$) are shown. They are in good agreement with the time evolutions provided by integration of a system of ordinary differential equations obtained by a Galerkin projection of Eqs. (4) and (5), using the first eight odd eigenfunctions as trial functions (Fig. 8).

5 Conclusions

An internally resonant elastic string is considered here under the action of an external harmonic force. A NES is engaged at a generic point of the string in order to reduce the amplitude of oscillations as a passive control device. The MSHBM, extended in order to deal with internally resonance cases, is applied in direct approach to the system of partial differential equations, to get amplitude modulation equations ruling the slow dynamics of the system.

Differently than the case with NES disengaged, where the dominant dynamics of the string is ruled just by the directly excited resonant mode, the presence of the NES involves (in a first approximation) both the resonant and a superharmonic components in the response, and amplitude modulation equations ruling the slow dynamics of them are coupled to the equation relevant to the NES slow amplitude of oscillation.

Numerical results for a case study are presented, denoting the contribution of both the components in periodic and quasiperiodic solutions, and the beneficial effect of the NES to reduce the amplitude of oscillation of the string. Results are in good agreement with those provided by a discrete, approximated, system of ordinary differential equations obtained by means of a Galerkin projection of the infinite dimensional problem.

Appendix: Coefficients of the equations

The expression of the right-hand sides of Eq. (31) is:

$$\mathcal{F}_1 = -\frac{\zeta}{2}a_r - \xi b\cos(\gamma-\vartheta)\sin(\omega_r x_C) + \frac{p_r}{\omega_r}\sin(\gamma) - \frac{3}{4\omega}\kappa b^3\sin(\gamma-\vartheta)\sin(\omega_r x_C)$$

The mass matrix of Eq. (31) is $\mathcal{M}(\mathbf{u}) =$

$$\begin{bmatrix} 1 & 0 & 0 & 0 & 0 & 0 \\ 0 & 1 & 0 & 0 & 0 & 0 \\ -m\omega_r \sin(\omega_r x_C)\cos(\gamma-\vartheta) & 0 & m\omega_r & m\omega_r a_r \sin(\omega_r x_C)\sin(\gamma-\vartheta) & 0 & -\frac{1}{2}\xi b \\ 0 & 0 & 0 & a_r & 0 & 0 \\ 0 & 0 & 0 & -3a_s & a_s & 0 \\ -m\omega_r \sin(\omega_r x_C)\sin(\gamma-\vartheta) & 0 & \frac{1}{2}\xi & -m\omega_r a_r \sin(\omega_r x_C)\cos(\gamma-\vartheta) & 0 & m\omega_r b \end{bmatrix} \tag{35}$$

$$\begin{aligned}
\mathcal{F}_2 &= -\frac{\zeta}{2}a_s - \frac{1}{4\omega}\kappa b^3 \sin(\omega_r x_C)\sin(3\gamma - 3\vartheta - \chi) \\
\mathcal{F}_3 &= -\frac{1}{2}\xi(\omega_r\sigma)b - \frac{1}{2}m x_C \xi \omega_r^2 b \sin(\omega_r x_C)\cos(\omega_r x_C) \\
&\quad + \frac{1}{2}m\xi\omega_r b \sin(\omega_r x_C)^2 \\
&\quad + m\omega_r(\omega_r+\sigma)a \sin(\omega_r x_C)\sin(\gamma-\vartheta) \\
&\quad - \frac{1}{2}m p_r \left[1 + (1 - x_C + x_C\cos(\omega_r))\cos(\omega_r x_C)\right. \\
&\quad \left. + \frac{1}{2\omega_r}(1-\cos(\omega_r))\sin(\omega_r x_C)\right]\sin(\vartheta) \\
&\quad + \frac{m\omega_r^4\omega_s^2}{32\omega_r^3 - 32\omega_r\omega_s^2}(\omega_s-\omega_r)a_r^2 a_s \\
&\quad \times \sin(\omega_r x_C)\sin(\gamma-\vartheta-\chi) \\
\mathcal{F}_4 &= a_r\sigma - \frac{3}{32}\eta\omega_r^3 a_r^3 - \frac{\eta}{16}\omega_r\omega_s^2 a_r a_s^2 + \frac{p_r}{\omega_r}\cos(\gamma) \\
&\quad - \frac{3}{4\omega_r}\kappa b^3 \sin(\omega_r x_C)\cos(\gamma-\vartheta) \\
&\quad + \xi b \sin\omega_r x_C)\sin(\gamma-\vartheta) \\
\mathcal{F}_5 &= -3\sigma a_s + \frac{\eta}{16}\omega_r\omega_s^2 _ r^2 a_s + \frac{3}{32\omega_r}\eta\omega_s^4 a_s^3 \\
&\quad + \frac{\kappa}{4\omega_r}b^3 \sin(\omega_r x_C)\cos(3\gamma - 3\vartheta - \chi) \\
\mathcal{F}_6 &= -m\omega_r\left(\frac{\omega_r}{2}+\sigma\right)b + \frac{3}{8}\kappa b^3 \\
&\quad - \frac{1}{2}m p_r x_C \left[1 - (1 - x_C + x_C\cos(\omega_r))\right. \\
&\quad \left. \times \cos(\omega_r x_C) - (1-\cos(\omega_r)\frac{\sin(\omega_r x_C)}{2\omega_r}\right]\cos(\vartheta) \\
&\quad + \frac{3}{8}m\kappa\omega_r x_C b^3 \cos(\omega_r x_C)\sin(\omega_r x_C) \\
&\quad + m\left(\sigma + \frac{\omega_r}{2}\right)\omega_r a_r \sin(\omega_r x_C)\cos(\gamma-\vartheta) \\
&\quad + \frac{m\omega_r^4\omega_s^2}{32\omega_r^3 - 32\omega_r\omega_s^2}(\omega_s-\omega_r)a_r^2 a_s \sin(\omega_r x_C) \\
&\quad \times \cos(\gamma-\vartheta-\chi) - \frac{3}{8}\kappa m b^3 \sin(\omega_r x_C)^2
\end{aligned} \tag{34}$$

References

1. Gattulli, V., Di Fabio, F., Luongo, A.: Simple and double Hopf bifurcations in aeroelastic oscillators with tuned mass dampers. J. Frankl. Inst. **338**, 187–201 (2001)
2. Gattulli, V., Di Fabio, F., Luongo, A.: One to one resonant double Hopf bifurcation in aeroelastic oscillators with tuned mass dampers. J. Sound Vib. **262**, 201–217 (2003)
3. Gattulli, V., Di Fabio, F., Luongo, A.: Nonlinear Tuned Mass Damper for self-excited oscillations. Wind Struct. **7**, 251–264 (2004)
4. Vakakis, A.F., Gendelman, O.V., Bergman, L.A., McFarland, D.M., Kerschen, G., Lee, Y.S.: Nonlinear Targeted Energy Transfer in Mechanical and Structural Systems. Springer, New York (2008)
5. Manevitch, L.: The description of localized normal modes in a chain of nonlinear coupled oscillators using complex variables. Nonlinear Dyn. **25**, 95–109 (2001)
6. Gendelman, O.V., Starosvetsky, Y., Feldman, M.: Attractors of harmonically forced linear oscillator with attached nonlinear energy sink I: Description of response regimes. Nonlinear Dyn. **51**, 31–46 (2008)
7. Starosvetsky, Y., Gendelman, O.V.: Dynamics of a strongly nonlinear vibration absorber coupled to a harmonically excited two-degree-of-freedom system. J. Sound Vib. **312**, 234–256 (2008)
8. Vaurigaud, B., Manevitch, L.I., Lamarque, C.-H.: Passive control of aeroelastic instability in a long span bridge model prone to coupled flutter using targeted energy transfer. J. Sound Vib. **330**, 2580–2595 (2011)
9. Gendelman, O.V., Vakakis, A.F., Bergman, L.A., McFarland, D.M.: Asymptotic analysis of passive nonlinear suppression of aeroelastic instabilities of a rigid wing in subsonic flow. SIAM J. Appl. Math. **70**(5), 1655–1677 (2010)
10. Costa, S.N.J., Hassmann, C.H.G., Balthazar, J.M., Dantas, M.J.H.: On energy transfer between vibrating systems under linear and nonlinear interactions. Nonlinear Dyn. **57**, 57–67 (2009)
11. Dantas, M.J.H., Balthazar, J.M.: On energy transfer between linear and nonlinear oscillators. J. Sound Vib. **315**, 1047–1070 (2008)
12. Felix, J.L.P., Balthazar, J.M., Dantas, M.J.H.: On energy pumping, synchronization and beat phenomenon in a non-ideal structure coupled to an essentially nonlinear oscillator. Nonlinear Dyn. **56**, 1–11 (2009)
13. Tusset, A.M., Balthazar, J.M., Chavarette, F.R., Felix, J.L.P.: On energy transfer phenomena, in a nonlinear ideal and

nonideal essential vibrating systems, coupled to a (MR) magneto-rheological damper. Nonlinear Dyn. **69**, 1859–1880 (2012)
14. Panagopoulos, P., Georgiades, F., Tsakirtzis, S., Vakakis, A.F., Bergman, L.A.: Multi-scaled analysis of the damped dynamics of an elastic rod with an essentially nonlinear end attachment. Int. J. Solids Struct. **44**, 6256–6278 (2007)
15. Georgiades, F., Vakakis, A.F.: Dynamics of a linear beam with an attached local nonlinear energy sink. Commun. Nonlinear Sci. Numer. Simul. **12**, 643–651 (2007)
16. Georgiades, F., Vakakis, A.F., Kerschen, G.: Broadband passive targeted energy pumping from a linear dispersive rod to a lightweight essentially non-linear end attachment. Int. J. Non-Linear Mech. **42**, 773–788 (2007)
17. Nili Ahmadabadi, Z., Khadem, S.E.: Nonlinear vibration control of a cantilever beam by a nonlinear energy sink. Mech. Mach. Theory **50**, 134–149 (2012)
18. Georgiades, F., Vakakis, A.F.: Passive targeted energy transfers and strong modal interactions in the dynamics of a thin plate with strongly nonlinear attachments. Int. J. Solids Struct. **46**, 2330–2353 (2009)
19. Zhang, Y.-W., Zang, J., Yang, T.-Z., Fang, B., Wen, X.: Vibration suppression of an axially moving string with transverse wind loadings by a nonlinear energy sink. Math. Probl. Eng. (2013). doi:10.1155/2013/348042
20. Malatkar, P., Nayfeh, A.H.: Steady-state dynamics of a linear structure weakly coupled to an essentially nonlinear oscillator. Nonlinear Dyn. **47**, 167–179 (2007)
21. Mehmood, A., Nayfeh, A.H., Hajj, M.R.: Effects of a nonlinear energy sink (NES) on vortex-induced vibrations of a circular cylinder. Nonlinear Dyn. **77**, 667–680 (2014)
22. Luongo, A., Zulli, D.: Dynamic analysis of externally excited NES-controlled systems via a mixed Multiple Scale/Harmonic Balance algorithm. Nonlinear Dyn. **70**(3), 2049–2061 (2012)
23. Luongo, A., Zulli, D.: Aeroelastic instability analysis of NES-controlled systems via a mixed Multiple Scale/Harmonic Balance Method. J. Vib. Control **20**(13), 1985–1998 (2014)
24. Gourc, E., Seguy, S., Michon, G., Berlioz, A.: Chatter control in turning process with a nonlinear energy sink. Diffus. Defect Data Pt.B Solid State Phenom. **201**, 89–98 (2013)
25. Bab, S., Khadem, S.A., Shahgholi, M.: Lateral vibration attenuation of a rotor under mass eccentricity force using nonlinear energy sink. Int. J. Non-Linear Mech. (2014). doi:10.1016/j.ijnonlinmec.2014.08.016
26. Zulli, D., Luongo, A.: Nonlinear energy sink to control vibrations of an internally nonresonant elastic string. Meccanica **50**, 781–794 (2015)
27. Nayfeh, A.H., Mook, D.T.: Nonlinear Oscillations. Wiley, New York (1979)
28. Nayfeh, S.A., Nayfeh, A.H., Mook, D.T.: Nonlinear response of a taut string to longitudinal and transverse end excitation. J. Vib. Control **1**(3), 307–334 (1995)
29. Rega, G., Lacarbonara, W., Nayfeh, A.H., Chin, C.M.: Multiple resonances in suspended cables: direct versus reduced-order models. Int. J. Non-Linear Mech. **34**, 901–924 (1999)
30. Lacarbonara, W.: Direct treatment and discretizations of non-linear spatially continuous systems. J. Sound Vib. **221**, 849–866 (1999)
31. Nayfeh, A.H., Nayfeh, S.A., Pakdemirli, M.: On the discretization of weakly nonlinear spatially continuous systems. In: Kliemann, W., Sri Namachchivaya, N. (eds.), Nonlinear Dynamics and Stochastic Mechanics, pp. 175–200. CRC Press, Boca Raton (1995)
32. Luongo, A., Zulli, D.: Mathematical Models of Beams and Cables. Iste-Wiley, ISBN 9781848214217 (2013)
33. Doedel, E.J., Oldeman, B.E.: AUTO-07P: Continuation and Bifurcation Software for Ordinary Differential Equation (2012). http://cmvl.cs.concordia.ca/auto/
34. Wolfram Research Inc.: Mathematica, Version 9.0. Wolfram Research Inc., Champaign (2012)
35. Ni, Y.Q., Wang, X.Y., Chen, Z.Q., Ko, J.M.: Field observations of rain-wind-induced cable vibration in cable-stayed Dongting Lake Bridge. J. Wind Eng. Ind. Aerodyn. **95**, 303–328 (2007)